Boundary-Layer Theory – 0540630901

Prof. H. Haustein

An analytical approximation of the wall-jet in a moving stream

By Krishanu Kumar

940673536

Abstract

The flow of a jet over a flat plate in the presence of a free stream is considered. The flow is essentially divided into two regions, upper and lower domain, based on the locus of maximum velocity U_{max}. The lower domain is approximated using the boundary layer equation proposed by Glauert (1956) for wall jet and also compared with Falkner-Skan's (1931) approximation for a flat plate. The upper region is simplified and solved as a heat conduction equation, based on Kashi and Haustein (2018). The theoretical approximation is then compared with the numerical simulation data. The approximation for the lower domain has good agreement with the numerical data and for the upper domain behaves similarly. For the upper domain, initial flow profile is essential in estimating the solution, however, in the present study an analytical function that resembles the flow profile is selected and development along the fetch is presented, which more or less agrees well with the numerical data.

Introduction

The wall jet is the flow flowing over a flat plate from a narrow slot. The laminar boundary layer equation governing the jet flow over a rigid wall was introduced by Glauert (1956), to possess similarity solution and have a closed solution. The compressible wall jet was discussed extensively by Riley (1958). The wall jet in the presence of moving base and suction was discussed in detail by Merkin and Needham (1986), Banks (1983), Mahmood (1988), and references therein. They found that the similarity solution exists for both the conditions if momentum along the flow is conserved, derived by Glauret (1956).

Eichelbrenner and Dumargue (1962) treated the plane, turbulent wall-jet in a moving stream of constant velocity. They separated the flow into two regions based on the position of maximum velocity and the two regions were joined at the maximum velocity height for the inner region and point of inflection in the outer region. Patel and Newman (1961), derived a simple set of similarity variables for the mean and turbulent flow, assuming the ratio of the maximum velocity and free-stream velocity remains constant. Experiments on a plane, steady, and turbulent wall jet with a negligible longitudinal pressure gradient in a constant free stream velocity, with varying velocity ratio were conducted by Erian and Eskinazi (1964), Kruka and Eskinazi (1964). They found that similarity exists in both inner and outer domains for mean and turbulent quantities, however, with different scaling parameters. Pantokratoras (2011), analysed the similarity solution of a wall jet along a moving base as well as in moving stream condition, based on the procedure proposed by Mahmood (1988).

In the present study, the flow is divided into two regions, the upper and lower region, based on the vertical position of maximum velocity; similar to Eichelbrenner and Dumargue (1962). The bottom half is solved using the boundary layer equation with boundary conditions as $f(0)=0$, $f'(0)=0$, and $f'(1)=1.25$ i.e., $U_{max}/U_{\infty}=1.25$, as well as Falkner-Skan equation with the boundary layer thickness is defined by the height of the maximum velocity U_{max}, and U_{∞} is assumed to be the local U_{max} obtained from the simulation. For the upper region, the boundary layer equation is simplified into a heat conduction equation, based on Kashi and Haustein (2018),

assuming $v\partial u/\partial y << u\partial u/\partial x$. A trigonometric function ($F(y,0) = sech^2(20y)$) is used as the initial function, which resembles the flow, to obtain an analytical solution; for more details see Carslaw and Jaeger (1956), and boundary conditions are prescribed as $F(0,x)=1$ and $F(1,x)=0$. The development of the flow based on the heat conduction equation resembles the flow development along the fetch estimated using numerical modeling. Both the theoretical approximations are compared with the results obtained from the numerical model.

Governing Equation

A typical example of the velocity profile is presented in Fig. 1. The flow regime is divided into two sub-regions: lower and upper regions. For the lower region, a two-dimensional laminar wall jet at $x=0$, is assumed with the wall in positive x-direction with uniform jet velocity U_j and a constant free-stream velocity U_∞. The equations of the governing flow are:

$$\frac{\partial u}{\partial x} + \frac{\partial v}{\partial y} = 0$$

$$u\frac{\partial u}{\partial x} + v\frac{\partial u}{\partial y} = \nu\frac{\partial^2 u}{\partial y^2}$$

with boundary conditions

$$u = 0, v = 0 \; at \; y = 0 \text{ and } u \to U_\infty \text{ as } y \to \infty$$

where y is the coordinate normal to the wall, with u and v the velocity component in x- and y-directions respectively. Based on Glaurt (1956), the equation is reduced to the following form:

$$f''' + ff'' + 2f'^2 = 0$$

with boundary condition $f(0)=0$ and $f'(0)=0$ and a modified boundary condition which represents the velocity ratio at $\eta/\eta_{max}=1$, given as $f'(1)=1.25$ is prescribed.

Similarly, the flat plate equation is given as: Falkner-Skan (1931)

$$f''' + \frac{1}{2}ff'' = 0$$

with boundary condition as $f(0)=0$, $f'(0)=0$, and $f'(\infty)=1$. An assumption is made that the maximum velocity U_{max} at the centreline represents the local free-stream velocity U_∞ in the equation Note that, the maximum velocity is reached at $\eta\approx5$, hence the normalised boundary layer thickness η/η_{max} is used for further analysis.

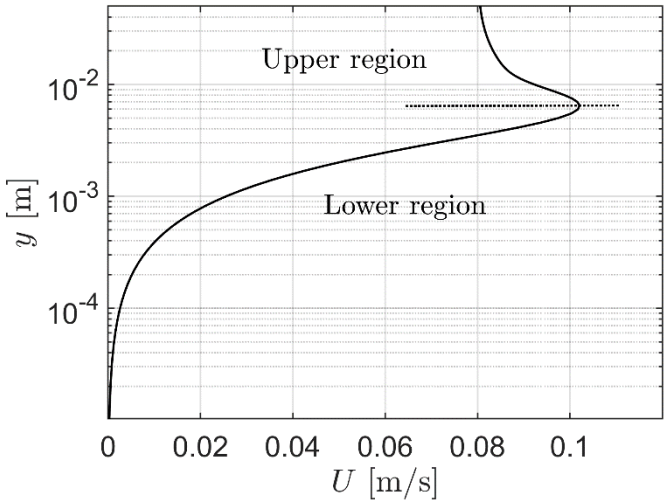

Fig. 1: Initial velocity profile of the flow; upper and lower region is separated by the dashed line at the height corresponding to maximum velocity U_{max}.

For the upper domain, the non-dimensional Navier-Stokes equation is used,

$$u\frac{\partial u}{\partial x} + v\frac{\partial u}{\partial y} = \frac{1}{Re}\frac{\partial^2 u}{\partial y^2}$$

where u and v are the velocity component in x- and y- directions respectively. For high Reynolds number u is assumed to be $>>v$ and the second term in the equation RHS can be neglected, hence, it is assumed near the maximum velocity height i.e., at $y' \to 0$, $v \to 0$, and $\partial u/\partial y \to 0$. Therefore, the vertical convection term is neglected simplifying the above equation as:

$$u\frac{\partial u}{\partial x} = \frac{1}{Re}\frac{\partial^2 u}{\partial y^2} \text{ or, } \frac{1}{2}\frac{\partial u^2}{\partial x} = \frac{1}{Re}\frac{\partial^2 u}{\partial y^2}$$

Substituting u^2 as f in the above equation,

$$\frac{1}{2}\frac{\partial f}{\partial x} = \frac{1}{Re}\frac{\partial^2 \sqrt{f}}{\partial y^2}$$

The equation can be further simplified using chain expansion i.e., $\frac{\partial^2 \sqrt{f}}{\partial y^2} = -\frac{1}{2}\frac{\partial}{\partial y}\left(\frac{1}{\sqrt{f}}\frac{\partial f}{\partial y}\right)$ and using linear type approximation, i.e., the x-direction velocity u is considered only a function of x i.e., $\sqrt{f}=u_c(x)$.

$$\frac{\partial f}{\partial x} = -\frac{1}{Re}\frac{1}{u_c(x)}\frac{\partial}{\partial y}\left(\frac{\partial f}{\partial y}\right) = -\frac{1}{Re_c(x)}\frac{\partial}{\partial y}\left(\frac{\partial f}{\partial y}\right)$$

where $Re_c(x)=Reu_c(x)$ and a non-linear stretching assumption on x-direction is made i.e., $X=x/Re_c(x)$, resulting in simplification of boundary layer equation for the upper domain as a simple heat conduction equation:

$$\frac{\partial f}{\partial X} = -\frac{\partial}{\partial y}\left(\frac{\partial f}{\partial y}\right)$$

The remaining assumptions are made based on Kashi and Haustein (2018), and with boundary conditions mentioned in the prequel section, and final form of analytical solution is obtained (Carlsaw and Jaeger (1959)):

$$F(X,y) = 1 - y + \left(\sum_{n=1}^{\infty} 2e^{-\pi^2 n^2 X} \sin(n\pi y)\left(\int_0^1 \frac{\sin(n\pi y)\left(1+(y-1)\cosh^2(20y)\right)}{\cosh^2(20y)} dy\right)\right)$$

Computational model and Boundary conditions

The geometry is created using commercial software, Ansys®, see Fig. 2. The length and height of the domain are taken as 0.5m and 0.25m respectively. The width of the jet is kept at around 0.005m. For flow boundary conditions, a uniform velocity is applied at the both free-stream and jet inlet. A pressure outlet is applied at the outlet of the domain, with top as symmetry and the bottom part as a wall, with a no-slip boundary condition. The flow inside the domain is assumed to be fully developed and the velocity at the wall is assumed to be zero. The laminar model is employed to solve the problem numerically, for more detail see Ansys 2018 manual.

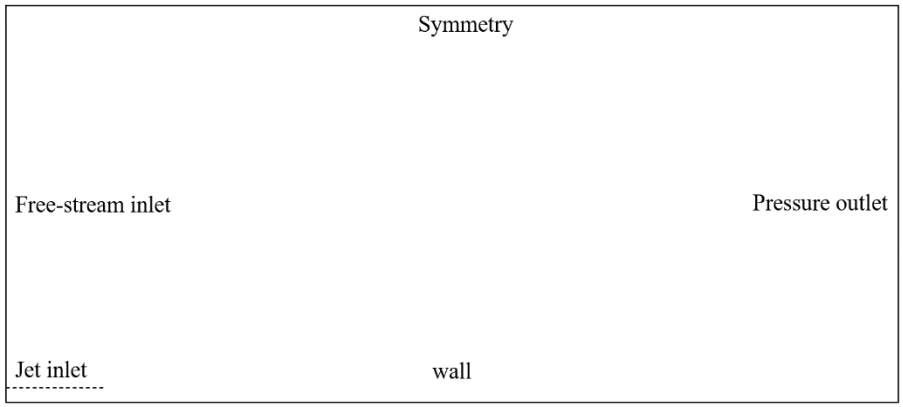

Fig. 2: Schematic of the numerical model with boundary condition.

The domain is then created with structured mesh in workbench with multi-domain method, see Fig. 3. The domain near the wall is given an inflation layer thickness to maintain wall $y^+ \leq 1$. A grid independence study was performed and a hybrid size ranging from 0.01 mm to 0.2mm was chosen to model the flow, maintaining orthogonal quality close to 1 and skewness close to zero. The fluent solves the laminar equation using the finite volume discretization method. Simple algorithm is applied for pressure-velocity coupling and momentum and energy conservation equations are solved by the second order-upwind method. The convergence limit for all quantities was kept around 1×10^{-4}.

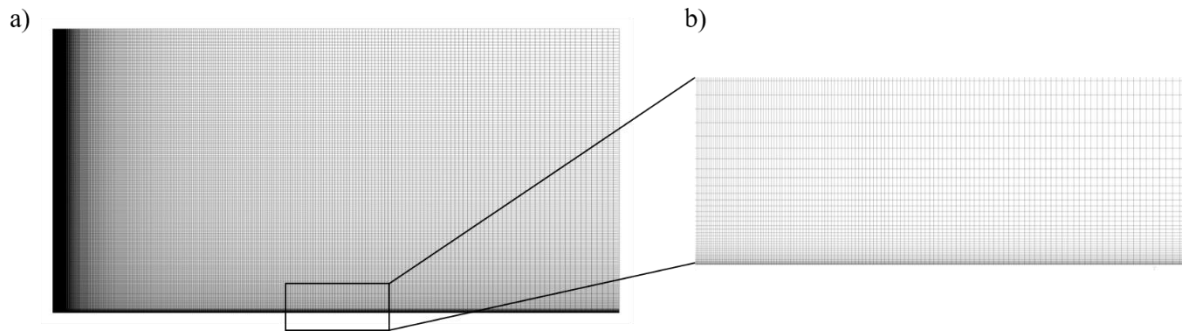

Fig. 3: Mesh generation in a) full domain and b) zoomed in-view near the wall.

Results and Discussion

The variation of velocity $U(y)$ in the y-direction is presented in Fig. 4, at different fetches. Note that the maximum velocity U_{max} decreases along the fetch and the distance of the peak velocity from the wall y_{max} increases. To compare the theoretical curve and the numerical data, the velocity in the lower domain is normalised by the peak velocity U_{max} and y is normalised by y_{max}, see Fig. 4b. For the upper domain, initially the velocity is subtracted by free-stream velocity and then normalised by (U_{max}-U_∞) and y is normalised by the position where the normalised velocity reaches 0.05, see Fig. 4c.

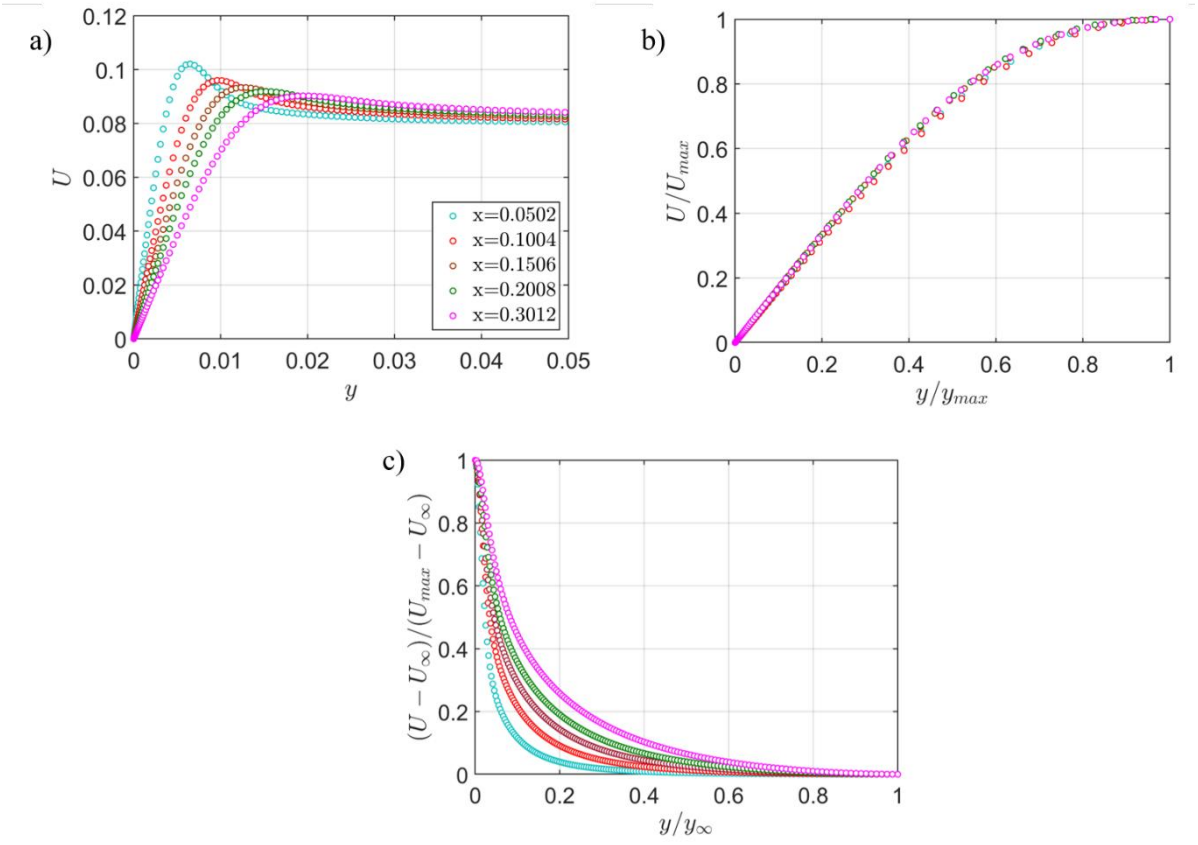

Fig. 4: a) Velocity profile $U(y)$ along the fetch, normalised velocity profile U/U_{max} for b) lower region, and c) upper region.

For the lower region, the comparison with theoretical approximation is presented in Fig. 5. The similarity function based on Glauert (1956) is presented by the **blue** line, which overestimates the velocity at $y/y_{max}>0.1$ when compared to numerical data. However, the curve estimated from Falkner-Skan's (1931) equation; the **black** line, agrees well with the numerical data. Note that, the free-stream velocity in Falkner-Skan approximation is assumed to be the local maximum velocity U_{max}. To compare the results, in the Figure boundary thickness is normalised by η_{max}.

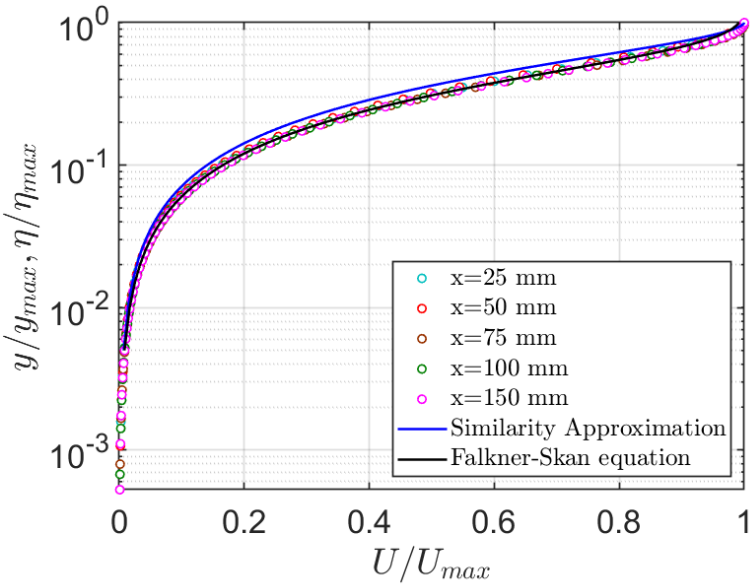

Fig. 5: Normalised velocity profile U/U_{max} of the lower region; **blue**: Similarity approximation by Glauret (1956), **black**: Falkner-Skan (1931).

For the upper domain, the transformed non-dimensional velocity profile is presented in Fig. 6a and a trigonometric function, $sech^2(20y)$ is selected as an initial function that approximately resembles the initial flow profile, refer Fig. 6b. Note that, the heat equation behaves similarly as the main velocity profile, however, it is not a perfect match because of the selected initial function. A trigonometric function was selected to obtain an analytical solution of the heat conduction equation, as discussed in the above section. It can predict the flow behavior appropriately, indicating the validity of the procedure. The heat equation solution is presented for values of X which is close to the actual position of numerical simulation, with x=25 mm as the starting position.

However, there is no interconnection between these two regions except the ending and starting position of both the regions. To predict the profile relaxation, the variation of both maximum velocity U_{max} and locus of U_{max}, (x,y_{max}) is essential which is extracted from the numerical simulation. Then the two regions can be joined at the maximum velocity height for the inner region and point of inflection in the outer region, similar to Eichelbrenner and Dumargue (1962).

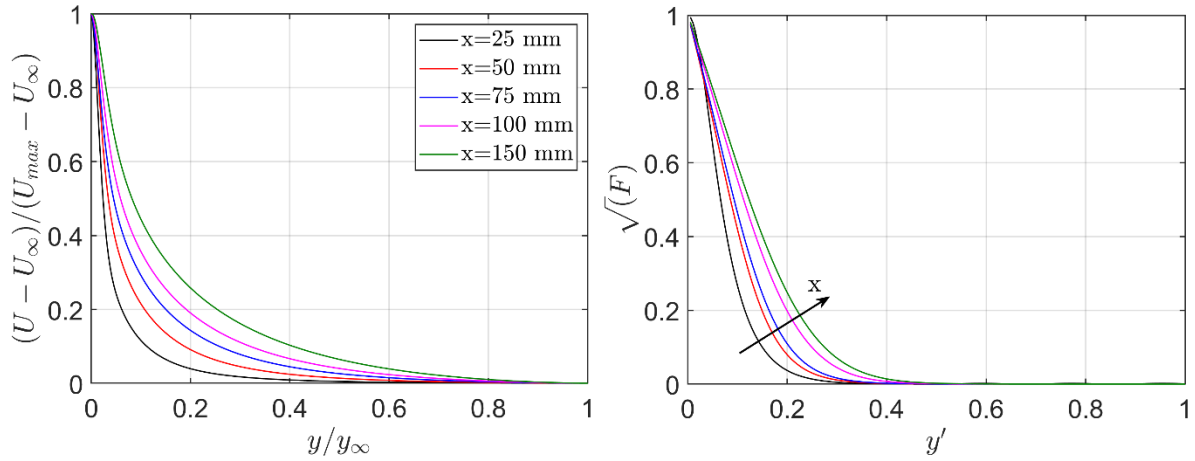

Fig. 6: Normalised velocity profile U/U_{max} of the upper region a) numerical data and b) solution obtained from heat conduction equation.

Conclusion

Many experiments and analytical solutions have been developed for free jet, wall jet, wall-jet with suction/blowing wall, and turbulent wall-jet (Glauert (1956), Riley (1958), Banks (1983), Mahmood (1988), Kruka and Eskinazi (1964) and references therein). Pantokratoras (2011) made an effort to present a complete set of results for the moving plate case as well as the mechanics of laminar wall jet in a free-stream combined with moving plate, based on numerical method derived by Mahmood (1988). In the present analysis, an effort has been made to implement a new approach by dividing the flow into two separate regions (lower and upper) and solving them separately; lower region with wall-jet and flat plate equation and upper region with heat conduction equation with appropriate boundary conditions. The flow is divided into two regions based on the position of maximum velocity U_{max}.

For the lower region, the boundary layer equation is solved as a normal wall jet, developed by Glauert (1956), with modified boundary conditions and Falkner-Skan's (1931) equation, with an assumption that the local maximum velocity U_{max} is equivalent to the free-stream velocity U_∞ in the equation. The wall-jet solution overpredicts the velocity, however, the flat-plate equation predicts the velocity accurately, indicating, when normalised appropriately, the normalised velocity profile for the lower regions falls on a single flat plate profile.

For the upper region, the vertical convection term is neglected to simplify the boundary layer equation into a simple heat conduction equation, Kashi and Haustein (2018). To obtain rather a simple analytical solution, instead of an actual curve, a trigonometric function resembling the actual profile is selected and is presented in Section above. The solution obtained from the heat equation at different X also resembles the actual flow profile and behaves similarly.

The results of the investigation of flow under consideration are satisfactory and seem to exhibit similar behavior as the main flow. However, further study and development of the equation at different Reynolds numbers have to be carried out to generalise the following procedure.

Acknowledgment

I would like to thank Prof Herman Haustein and Avishai Oved for several discussions and advice.

References

M. B. Glauert (1956) The wall jet, J. Fluid Mech. 1 625-643.

V.M. Falkneb B.Sc. and Miss S.W. Skan (1931) LXXXV. Solutions of the boundary-layer equations, The London, Edinburgh, and Dublin Philosophical Magazine and Journal of Science, 12:80, 865-896.

B. Kashi and H. D. Haustein (2018) Dependence of submerged jet heat transfer on nozzle length, Int. J. Heat Mass Transf. 121, 137-152.

N. Riley (1958) Effects of compressibility on a laminar wall jet, J. Fluid Mech. 4, 615-628.

J. H. Merkin and D. J. Needham (1986) A note on wall-jet problem, J. Eng. Math. 20, 21-26.

W. H. H. Banks (1983) Similarity solutions of the boundary-layer equations for a stretching wall. J. de Mecanique theorique et appliquee, 2, 375-392.

T. Mahmood (1988) A laminar wall jet on a moving wall, Acta Mech., 71, 51–60.

A. Eichelbrenneer and P. Dumargue, (1962) The problem of the plane turbulent wall jet with an external flow of constant velocity, J. Mecanique, 1, 109.

R. P. Patel and B. G. Newman (1961) Self-preserving two-dimensional jets and wall jets in a moving stream, McGill Univ Rep. Ae, 5.

F. Erian and S. Eskinazi (1964) The wall-jet in a longitudinal pressure gradient, Geology.

V. Kruka and S. Eskinazi (1964) The wall-jet in a moving stream, J. Fluid Mech., 20, 555-579.

A. Pantokratoras (2011) The nonsimilar laminar wall jet along a moving wall, in a free stream and in a free stream/moving wall, Appl. Math. Model, 35, 471-481.

H. S. Carslaw and J. C. Jaeger (1956) Conduction of heat in solids, Oxford Science Publications.

Derivation of Glauret (1956) equation:

restart :

$$\mathrm{eta}(x,y) = \left(\frac{U}{\mathrm{nu}\cdot x^3}\right)^{\frac{1}{4}}\cdot y$$

$$\eta(x,y) = \left(\frac{U}{\nu\, x^3}\right)^{1/4} y \tag{1}$$

differentiate w.r.t. y →

$$\frac{\partial}{\partial y}\,\eta(x,y) = \left(\frac{U}{\nu\, x^3}\right)^{1/4} \tag{2}$$

$$\eta(x,y) = \left(\frac{U}{\nu\, x^3}\right)^{1/4} y \xrightarrow{\text{differentiate w.r.t. x}} \frac{\partial}{\partial x}\,\eta(x,y) = -\frac{3\,y\,U}{4\left(\frac{U}{\nu\, x^3}\right)^{3/4}\nu\, x^4} \xrightarrow{\text{simplify symbolic}}$$

$$\frac{\partial}{\partial x}\,\eta(x,y) = -\frac{3\,U^{1/4}\,y}{4\,\nu^{1/4}\,x^{7/4}}$$

$$\mathrm{psi}(x,y) = 4\cdot\mathrm{nu}\cdot\left(\frac{U\cdot x}{\mathrm{nu}}\right)^{\frac{1}{4}}\cdot f(\mathrm{eta}(x,y)) \xrightarrow{\text{simplify symbolic}} \psi(x,y) = 4\,U^{1/4}\,\nu^{3/4}\,x^{1/4} f(\eta(x,y))$$

$$\psi(x,y) = 4\,U^{1/4}\,\nu^{3/4}\,x^{1/4} f(\eta(x,y))$$

$$\psi(x,y) = 4\,U^{1/4}\,\nu^{3/4}\,x^{1/4} f(\eta(x,y)) \tag{3}$$

differentiate w.r.t. y →

$$\frac{\partial}{\partial y}\,\psi(x,y) = 4\,U^{1/4}\,\nu^{3/4}\,x^{1/4}\,\mathrm{D}(f)\,(\eta(x,y))\left(\frac{\partial}{\partial y}\,\eta(x,y)\right) \tag{4}$$

$$\frac{\partial}{\partial y}\,\psi(x,y) = 4\,U^{1/4}\,\nu^{3/4}\,x^{1/4}\,\mathrm{D}(f)\,(\eta(x,y))\left(\left(\frac{U}{\nu\, x^3}\right)^{1/4}\right)$$

$$\frac{\partial}{\partial y}\,\psi(x,y) = 4\,U^{1/4}\,\nu^{3/4}\,x^{1/4}\,\mathrm{D}(f)\,(\eta(x,y))\left(\frac{U}{\nu\, x^3}\right)^{1/4} \tag{5}$$

simplify symbolic →

$$\frac{\partial}{\partial y}\,\psi(x,y) = \frac{4\sqrt{U}\,\sqrt{\nu}\,\mathrm{D}(f)\,(\eta(x,y))}{\sqrt{x}} \tag{6}$$

differentiate w.r.t. y →

$$\frac{\partial^2}{\partial y^2}\,\psi(x,y) = \frac{4\sqrt{U}\,\sqrt{\nu}\,\mathrm{D}^{(2)}(f)\,(\eta(x,y))\left(\frac{\partial}{\partial y}\,\eta(x,y)\right)}{\sqrt{x}} \tag{7}$$

$$\frac{\partial^2}{\partial y^2}\,\psi(x,y) = \frac{4\sqrt{U}\,\sqrt{\nu}\,\mathrm{D}^{(2)}(f)\,(\eta(x,y))\left(\left(\frac{U}{\nu\, x^3}\right)^{1/4}\right)}{\sqrt{x}}$$

$$\frac{\partial^2}{\partial y^2}\,\psi(x,y) = \frac{4\sqrt{U}\sqrt{\nu}\,D^{(2)}(f)\left(\eta(x,y)\right)\left(\frac{U}{\nu x^3}\right)^{1/4}}{\sqrt{x}} \tag{8}$$

simplify symbolic →

$$\frac{\partial^2}{\partial y^2}\,\psi(x,y) = \frac{4\,U^{3/4}\nu^{1/4}D^{(2)}(f)\left(\eta(x,y)\right)}{x^{5/4}} \tag{9}$$

differentiate w.r.t. y →

$$\frac{\partial^3}{\partial y^3}\,\psi(x,y) = \frac{4\,U^{3/4}\nu^{1/4}D^{(3)}(f)\left(\eta(x,y)\right)\left(\frac{\partial}{\partial y}\,\eta(x,y)\right)}{x^{5/4}} \tag{10}$$

$$\frac{\partial^3}{\partial y^3}\,\psi(x,y) = \frac{4\,U^{3/4}\nu^{1/4}D^{(3)}(f)\left(\eta(x,y)\right)\left(\left(\frac{U}{\nu x^3}\right)^{1/4}\right)}{x^{5/4}}$$

$$\frac{\partial^3}{\partial y^3}\,\psi(x,y) = \frac{4\,U^{3/4}\nu^{1/4}D^{(3)}(f)\left(\eta(x,y)\right)\left(\frac{U}{\nu x^3}\right)^{1/4}}{x^{5/4}} \tag{11}$$

simplify symbolic →

$$\frac{\partial^3}{\partial y^3}\,\psi(x,y) = \frac{4\,U D^{(3)}(f)\left(\eta(x,y)\right)}{x^2} \tag{12}$$

$$\frac{\partial}{\partial y}\,\psi(x,y) = \frac{4\sqrt{U}\sqrt{\nu}\,D(f)\left(\eta(x,y)\right)}{\sqrt{x}} \xrightarrow{\text{differentiate w.r.t. x}}$$

$$\frac{\partial^2}{\partial x\partial y}\,\psi(x,y) = -\frac{2\sqrt{U}\sqrt{\nu}\,D(f)\left(\eta(x,y)\right)}{x^{3/2}} + \frac{4\sqrt{U}\sqrt{\nu}\,D^{(2)}(f)\left(\eta(x,y)\right)\left(\frac{\partial}{\partial x}\,\eta(x,y)\right)}{\sqrt{x}}$$

$$\frac{\partial^2}{\partial x\partial y}\,\psi(x,y) = -\frac{2\sqrt{U}\sqrt{\nu}\,D(f)\left(\eta(x,y)\right)}{x^{3/2}} + \frac{4\sqrt{U}\sqrt{\nu}\,D^{(2)}(f)\left(\eta(x,y)\right)\left(-\frac{3\,U^{1/4}y}{4\,\nu^{1/4}x^{7/4}}\right)}{\sqrt{x}}$$

$$\frac{\partial^2}{\partial x\partial y}\,\psi(x,y) = -\frac{2\sqrt{U}\sqrt{\nu}\,D(f)\left(\eta(x,y)\right)}{x^{3/2}} - \frac{3\,U^{3/4}\nu^{1/4}D^{(2)}(f)\left(\eta(x,y)\right)y}{x^{9/4}} \tag{13}$$

simplify symbolic →

$$\frac{\partial^2}{\partial x\partial y}\,\psi(x,y) = -\frac{2\left(\frac{3\,D^{(2)}(f)\left(\eta(x,y)\right)U^{1/4}x^{1/4}y}{2} + D(f)\left(\eta(x,y)\right)x\nu^{1/4}\right)\nu^{1/4}\sqrt{U}}{x^{5/2}} \tag{14}$$

$$\psi(x,y) = 4\,U^{1/4}\nu^{3/4}x^{1/4}f\left(\eta(x,y)\right)$$

$$\psi(x,y) = 4\,U^{1/4}\nu^{3/4}x^{1/4}f\left(\eta(x,y)\right) \tag{15}$$

differentiate w.r.t. x →

$$\frac{\partial}{\partial x}\,\psi(x,y)=\frac{U^{1/4}\nu^{3/4}f(\eta(x,y))}{x^{3/4}}+4\,U^{1/4}\nu^{3/4}x^{1/4}\mathrm{D}(f)\left(\eta(x,y)\right)\left(\frac{\partial}{\partial x}\,\eta(x,y)\right) \tag{16}$$

$$\frac{\partial}{\partial x}\,\psi(x,y)=\frac{U^{1/4}\nu^{3/4}f(\eta(x,y))}{x^{3/4}}+4\,U^{1/4}\nu^{3/4}x^{1/4}\mathrm{D}(f)\left(\eta(x,y)\right)\left(-\frac{3\,U^{1/4}y}{4\,\nu^{1/4}x^{7/4}}\right)$$

$$\frac{\partial}{\partial x}\,\psi(x,y)=\frac{U^{1/4}\nu^{3/4}f(\eta(x,y))}{x^{3/4}}-\frac{3\sqrt{U}\sqrt{\nu}\,\mathrm{D}(f)\left(\eta(x,y)\right)y}{x^{3/2}} \tag{17}$$

simplify symbolic

$$\frac{\partial}{\partial x}\,\psi(x,y)=\frac{U^{1/4}\sqrt{\nu}\left(-3\,\mathrm{D}(f)\left(\eta(x,y)\right)x^{1/4}U^{1/4}y+f(\eta(x,y))\,x\,\nu^{1/4}\right)}{x^{7/4}} \tag{18}$$

$$\left(\frac{4\sqrt{U}\sqrt{\nu}\,\mathrm{D}(f)\left(\eta(x,y)\right)}{\sqrt{x}}\right)\cdot\left(-\frac{2\left(\frac{3\,\mathrm{D}^{(2)}(f)\left(\eta(x,y)\right)U^{1/4}x^{1/4}y}{2}+\mathrm{D}(f)\left(\eta(x,y)\right)x\,\nu^{1/4}\right)\nu^{1/4}\sqrt{U}}{x^{5/2}}\right.$$
$$\left.-\left(\frac{U^{1/4}\sqrt{\nu}\left(-3\,\mathrm{D}(f)\left(\eta(x,y)\right)x^{1/4}U^{1/4}y+f(\eta(x,y))\,x\,\nu^{1/4}\right)}{x^{7/4}}\right)\cdot\left(\frac{4\,U^{3/4}\nu^{1/4}\mathrm{D}^{(2)}(f)\left(\eta(x,y)\right)}{x^{5/4}}\right)=\mathrm{nu}\cdot\frac{4\,U\mathrm{D}^{(3)}(f)\left(\eta(x,y)\right)}{x^2}\right.$$
$$-\frac{8\,U\nu^{3/4}\mathrm{D}(f)\left(\eta(x,y)\right)\left(\frac{3\,\mathrm{D}^{(2)}(f)\left(\eta(x,y)\right)U^{1/4}x^{1/4}y}{2}+\mathrm{D}(f)\left(\eta(x,y)\right)x\,\nu^{1/4}\right)}{x^3} \tag{19}$$
$$-\frac{4\,U\nu^{3/4}\left(-3\,\mathrm{D}(f)\left(\eta(x,y)\right)x^{1/4}U^{1/4}y+f(\eta(x,y))\,x\,\nu^{1/4}\right)\mathrm{D}^{(2)}(f)\left(\eta(x,y)\right)}{x^3}$$
$$=\frac{4\,\nu\,U\mathrm{D}^{(3)}(f)\left(\eta(x,y)\right)}{x^2}$$

simplify symbolic

$$-\frac{4\,U\nu\left(2\,\mathrm{D}(f)\left(\eta(x,y)\right)^2+\mathrm{D}^{(2)}(f)\left(\eta(x,y)\right)f(\eta(x,y))\right)}{x^2}=\frac{4\,\nu\,U\mathrm{D}^{(3)}(f)\left(\eta(x,y)\right)}{x^2} \tag{20}$$

move to right

$$0=\frac{4\,\nu\,U\mathrm{D}^{(3)}(f)\left(\eta(x,y)\right)}{x^2}+\frac{4\,U\nu\left(2\,\mathrm{D}(f)\left(\eta(x,y)\right)^2+\mathrm{D}^{(2)}(f)\left(\eta(x,y)\right)f(\eta(x,y))\right)}{x^2} \tag{21}$$

simplify symbolic

$$0=\frac{4\,\nu\,U\left(2\,\mathrm{D}(f)\left(\eta(x,y)\right)^2+\mathrm{D}^{(2)}(f)\left(\eta(x,y)\right)f(\eta(x,y))+\mathrm{D}^{(3)}(f)\left(\eta(x,y)\right)\right)}{x^2} \tag{22}$$

```
restart :
ode := f''' + f·f'' + 2·f^2 = 0
```

$$ode := \frac{d^3}{dx^3} f(x) + f(x) \left(\frac{d^2}{dx^2} f(x) \right) + 2 \left(\frac{d}{dx} f(x) \right)^2 = 0 \quad \textbf{(23)}$$

```
bc := f(0) = 0, D(f)(0) = 0, D(f)(1) = 1.25
```

$$bc := f(0) = 0, D(f)(0) = 0, D(f)(1) = 1.25 \quad \textbf{(24)}$$

```
s := dsolve({bc, ode}, numeric)
```

$$s := \textbf{proc}(x\_bvp) \ \ldots \ \textbf{end proc} \quad \textbf{(25)}$$

```
with(plots) :
p := odeplot(s, [[diff(f(x), x), x]], 0..1)
```

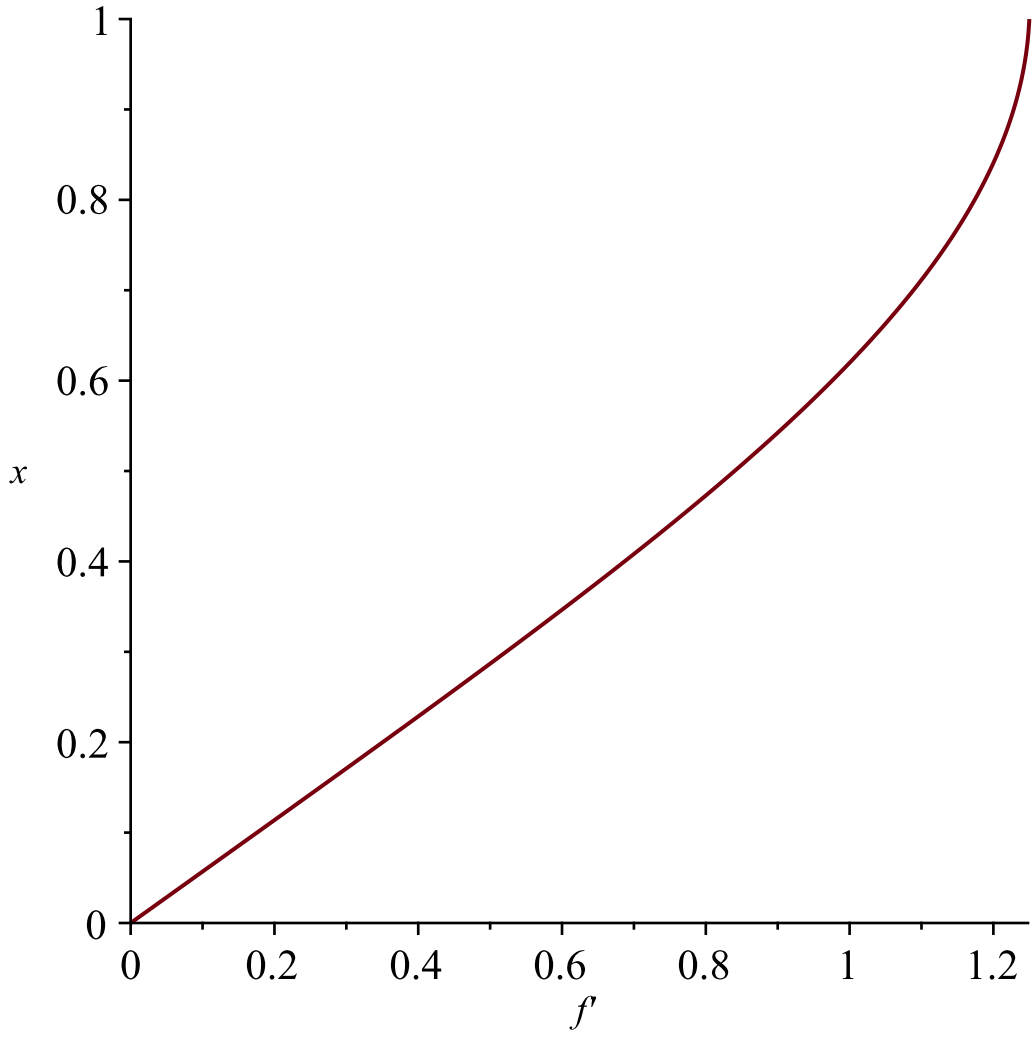

Heat conduction equation for upper region:

```
restart :
ode := diff(F(x, y), x) = diff(F(x, y), y, y)
```

$$ode := \frac{\partial}{\partial x} F(x, y) = \frac{\partial^2}{\partial y^2} F(x, y) \quad \textbf{(26)}$$

```
bc := F(0, y) = sech(20·y)^5, F(x, 0) = 1, F(x, 1) = 0
```

$$bc := F(0, y) = \operatorname{sech}(20\, y)^5, F(x, 0) = 1, F(x, 1) = 0 \quad \textbf{(27)}$$

$s := dsolve(\{bc, ode\}, F(x, y))$

$$s := F(x,y) = 1 - y + \left(\sum_{n=1}^{\infty} 2\, e^{-\pi^2 n^2 x} \sin(n\pi y) \left(\int_0^1 \frac{\sin(n\pi y)\,(1 + (y-1)\cosh(20y)^5)}{\cosh(20y)^5}\, dy \right) \right) \tag{28}$$